Synthesis of delafossite $CuCrO_2$ via solution combustion method and its acid functionalization for biodiesel production

*M. C. Viegas[1], G. P. de Figueredo[1], S. F. Rodrigues[2], A. A. Cabral[2], M. A. M. Castro[3], M. M. Oliveira[1]**
[1]*Instituto Federal do Maranhão, PPGQ/DAQ, Av. Getúlio Vargas 4, 65025-001, São Luís, MA, Brazil*
[2]*Instituto Federal do Maranhão, PPGEM, São Luís, MA, Brazil*
[3]*Universidade Federal do Rio Grande do Norte, PPGCEM, Natal, RN, Brazil*

Abstract

$CuCrO_2$ was synthesized by solution combustion synthesis (SCS) and applied as a heterogeneous catalyst to produce soybean biodiesel. The combustion reaction was carried out using urea as a fuel, and copper (II) and chromium (III) nitrates as precursors. After the powders' obtention, these were calcined and functionalized in an acidic medium. The powders were characterized by thermogravimetry (TG), X-ray diffraction (XRD), scanning electron microscopy (SEM), and infrared spectroscopy (IR) techniques. The TG curve revealed that the formation of the $CuCrO_2$ in the combustion reaction remained stable up to 1000 °C. The XRD results confirmed the formation of the $CuCrO_2$ compound. The SEM images showed that the crystallinity of the samples increased after the calcination process. The IR spectra showed the presence of delafossite characteristic bands. After the transesterification reaction, biodiesel was obtained with a yield of around 80%. Thus, catalysts based on delafossite synthesized through the combustion method and functionalized showed to be promising for the transesterification reaction of vegetable oils.
Keywords: delafossite, solution combustion synthesis, heterogeneous catalyst, transesterification reaction.

INTRODUCTION

Delafossites are a class of minerals formed by ternary oxides that present a general formula of the type ABO_2, where A and B represent metallic cations [1]. The A elements have a 1^+ charge (such as Cu, Pt, and Ag), while the B elements have a 3^+ charge (Fe, Cr, Al, and Ga being more common) [1, 2]. These compounds have a crystalline structure of hexagonal or rhombohedral type displayed in layer forms. Additionally, their arrangement depends on the type of orientation that each layer is disposed of in the compound structure [3]. The layers are formed by A^+ cations-bound oxygen, which forms O-A-O. These are coupled to the BO_6 octahedron that is formed by the trivalent ions B^{3+} bonded to the oxygen atoms [3, 4]. Delafossite $CuCrO_2$ is an oxide semiconductor that has excellent electrical, magnetic, and optical properties. The oxide is used mainly to produce electrodes and sensors for the photocatalysis process and other applications [1-5]. This material is also widely studied for transparent conducting oxide (TCO) applications due to its unique combination of electrical conductivity and optical transparency [5, 6]. These properties are directly related to its particle size and surface characteristics, which mainly depend on the synthesis process. Some ceramic powder synthesis method details can be found in the literature [7]. It is worth highlighting the solution combustion synthesis that stands out for its versatility, simplicity, cost, and process speed. It has been shown that this method led to particles that present good chemical homogeneity results [7, 8].

Compounds based on $CuCrO_2$ are promising for application in heterogeneous catalytic systems, such as the transesterification process to produce biodiesel. In such a process, a basic or acidic catalyst is used to improve the reaction rate and yield. On the other hand, when mainly homogeneous basic catalysts (NaOH and KOH) are used [9-11], the presence of these compounds leads to the contamination of the final product, which requires expensive washing and refining steps. Instead, heterogeneous acid catalysts do not present these problems and are still able to be recycled and reused for new reactions [9-12]. The performance of $CuCrO_2$ for the transesterification of vegetable oils can be significantly improved by increasing its acidic character. This is a requirement to subject it to a chemical functionalization in an acidic medium [13-15]. According to Zhong et al. [16], functionalization modifies the surface of the solid, promoting the addition of acid sites that remove impurities and decrease the hydrophobicity.

In this study, ceramic powders based on delafossite $CuCrO_2$ were obtained using the solution combustion method. This was followed by chemical functionalization in order to verify its behavior as a heterogeneous catalyst for the production of biodiesel from soybean oil. It is noteworthy that the solution combustion method is a cheap method in terms of energy expenditure, as it takes advantage of the heat of the reaction to synthesize the material and the reagents involved in the process have relatively low cost.

EXPERIMENTAL

Synthesis of delafossite by solution combustion method (SCS): the ceramic powders were synthesized by combustion reaction, using metallic nitrates as precursors and urea as fuel. To obtain 5 g (0.034 mol) of delafossite

**marcelo@ifma.edu.br*
https://orcid.org/0000-0003-4991-8157

$CuCrO_2$, stoichiometric quantities of the reagents were used as follows: 8.18 g (0.034 mol) of copper nitrate [$Cu(NO_3)_2.3H_2O$, Isofar], 13.56 g (0.034 mol) of chromium nitrate [$Cr(NO_3)_3.9H_2O$, Sigma Aldrich] and 8.47 g (0.141 mol) of urea [$(NH_2)_2CO$, Synth], all of them of analytical grade. The mixture of reagents (in 20 mL of deionized water) was previously heated at ~65 ℃ and stirred in a magnetic stirrer until an emulsion was formed. Then, the mixture was taken into a muffle furnace, heated to 400 °C, and held there for 10 min for the total completion of the reaction. The powder resulting from the reaction was deagglomerated in an agate mortar, heated at a rate of 10 °C.min^{-1} to be calcined at 1100 °C for a period of 2 h in a muffle furnace.

Functionalization: after the synthesis process, a part of the powder was functionalized in an acidic medium. The employed chemical treatment was carried out according to the methodology shown elsewhere [16]. Initially, 250 mL of a solution 1 mol.L^{-1} of H_2SO_4 (>95%, Merck) was prepared. Then, 100 mL of the H_2SO_4 solution was transferred to a flat bottom flask, to which 1.0 g of the obtained oxide ($CuCrO_2$) was added. For this treatment, a reflux system was installed using a magnetic stirring with a heater. The mixture was kept in this apparatus at a temperature range of approximately 80 °C for 2 h. After this period, the mixture was filtered, washed with deionized water up to pH=5.0, and dried in an oven at 100 °C for 4 h. Table I shows the identification of the non-calcined, calcined, and functionalized samples, and their corresponding obtaining temperatures.

Table I - Identification code of the samples.

Description	Temperature (°C)	Sample
Non-calcined	400	$CuCrO_2$-NC
Calcined	1100	$CuCrO_2$-CC
Functionalized	1100	$CuCrO_2$-FC

Transesterification reaction: for this reaction, refined soybean oil and ethanol were used as reagents for biodiesel production. The reactions were conducted by using 5% in mol of the functionalized catalyst in relation to the oil mass (0.5 g), alcohol:oil molar ratio of 12:1 (38 mL of ethanol:50 mL of oil) at 150 °C during 6 h of reaction in a reactor (4848, Parr). The reaction was kept under constant agitation while the soybean biodiesel was obtained. The biodiesel composition was analyzed through the gas chromatography technique. The reaction yield was calculated according to:

$$\text{Yield } (\%) = \frac{M_{biodiesel}}{M_{oil}} .100 \quad \text{(A)}$$

where $M_{biodiesel}$ represents the obtained biodiesel mass and M_{oil} is the soybean oil mass used in the reaction [17]. Analyzes of the biodiesel were also carried out by gas chromatography (GC) in order to evaluate the conversion rate of triglycerides to alkyl esters. The experiments were carried out in a gas chromatograph analyzer (CG-2010, Shimadzu), coupled with a mass spectrometer (CG-EM QP2010 Plus, Shimadzu). A capillary column (30 m x 0.25 mm x 0.25 μm, ZB-FFAP, Phenomenex) with a flow of carrier gas (He) at a linear speed of 47.5 cm.s^{-1} and column flow of 1.0 mL.min^{-1} was used.

Characterizations: the samples were characterized by thermogravimetry (TG), X-ray diffraction (XRD), scanning electron microscopy (SEM), infrared spectroscopy (IR), and gas chromatography (GC). TG was carried out so that variations in the mass of the compound $CuCrO_2$ as a function of temperature were observed. The analyzes were carried out in a thermal analyzer (STA 409, Netzsch) by the dynamic method of analysis with a heating rate of 10 °C.min^{-1} in static air and at a temperature range of 25 to 1000 °C. The XRD characterization was performed to determine the structure and crystalline phases presented in the samples. The technique was done by using an X-ray diffractometer (XRD-6100, Shimadzu), with CuKα radiation (1.5406 Å), scanning speed of 2 °.min^{-1}, and angle of 2θ from 10° to 80°. SEM was employed to analyze the morphological characteristics of the sample surfaces. The analyzes were carried out using a microscope (Vega3 LMU, Tesca) in secondary electron mode. The identification and characterization of the groups present in the samples were carried out by infrared absorption spectroscopy. For this, a spectrophotometer (Prestige 2, Shimadzu) was used. Here, the transmittance spectra of the samples were obtained in a range of 4000 to 400 cm^{-1}, resolution of 4 cm^{-1}, and an average of 40 scans.

RESULTS AND DISCUSSION

Thermogravimetry (TG): the thermogravimetric curves obtained from the $CuCrO_2$-NC sample are shown in Fig. 1a and TG/DSC in Fig. 1b. It is possible to observe in Fig. 1a that there was a small loss in mass of the material, less than 1%, as the temperature varied. This showed that the synthesis proved to be efficient because it was possible to obtain a stable material. Nevertheless, three distinct events are shown in Fig. 1b, evidenced by the peaks in the DSC (differential scanning calorimetry) curve. In region I, the initial mass loss was due to the loss of water that is part of the delafossite structure [18, 19]. In regions II and III (600 and 800 °C, respectively), the mass loss process may be associated with the elimination of organic residues formed during the synthesis, derived from urea [20].

X-ray diffraction (XRD): the diffractograms obtained for the non-calcined ($CuCrO_2$-NC), calcined ($CuCrO_2$-CC), and functionalized ($CuCrO_2$-FC) samples are depicted in Fig. 2. The delafossite phase was obtained for the three analyzed samples, but with different diffraction profiles. For the non-calcined sample (NC), the formation of the delafossite phase occurred with the presence of secondary phases such as Cr_2O_3 (PDF 038-1479) and CuO (PDF 041-0254). The functionalized sample ($CuCrO_2$-FC) exhibited a similar profile when compared to the non-calcined material, also with the presence of secondary phases. In the calcined sample

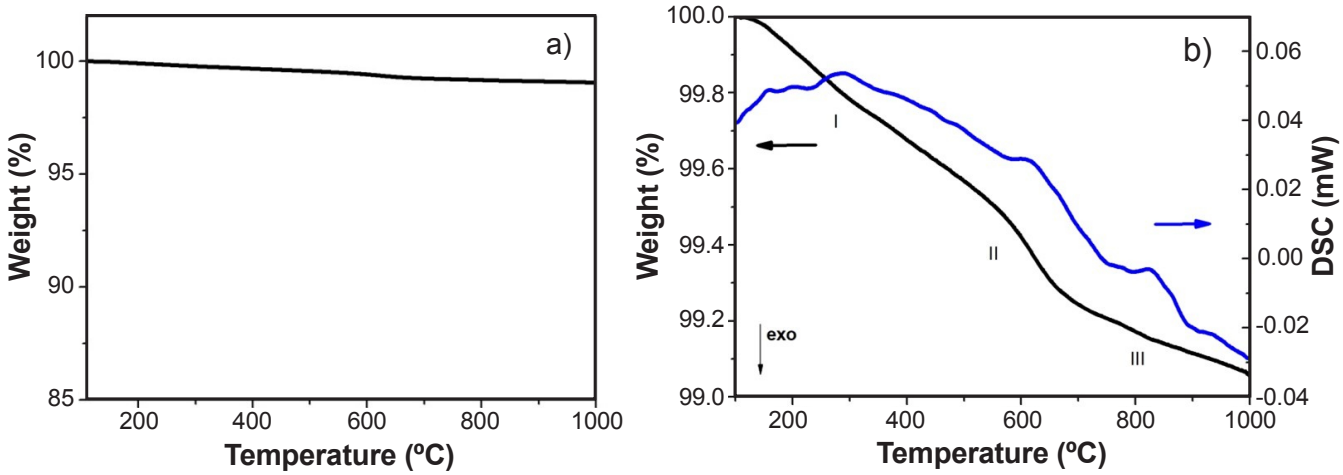

Figure 1: Thermogravimetric curves of $CuCrO_2$-NC sample: a) original curve; and b) scale enlargement of TG/DSC curves.

($CuCrO_2$-CC), the pure phase of delafossite (PDF 039-0247), of rhombohedral structure (R-3M), was observed. According to Martins et al. [21], the increase of the calcination temperature up to 1100 °C favors the transition from the secondary phases to the $CuCrO_2$. Furthermore, chemical functionalization in an acidic medium may result in structural defects of the compounds which lead to the conversion of Cu and Cr oxides during the acidification process [22, 23]. The high-intensity peaks in relation to the $CuCrO_2$-NC material were due to the fact that the $CuCrO_2$-FC sample was previously calcined.

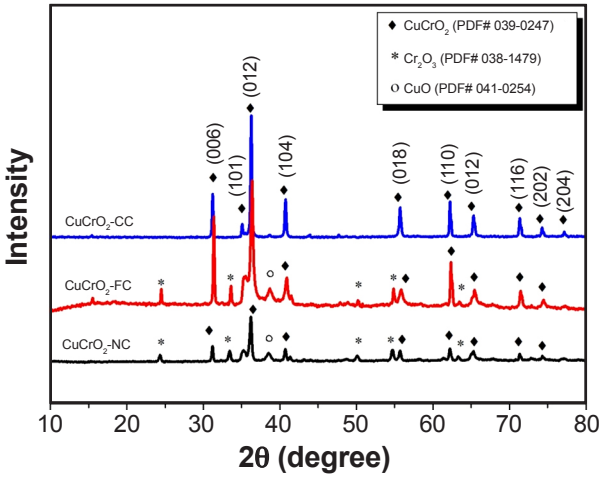

Figure 2: X-ray diffractograms of $CuCrO_2$ samples: $CuCrO_2$-NC, $CuCrO_2$-FC, and $CuCrO_2$-CC.

Scanning electron microscopy (SEM): the morphologies of the $CuCrO_2$ compound before and after heat treatment are shown in Figs. 3a and 3b, respectively. It was possible to observe a clear difference in the morphology and particle sizes. The $CuCrO_2$-NC sample showed a pronounced porous appearance, with poorly defined particle morphology. On the other hand, the $CuCrO_2$-CC sample exhibited a more homogeneous morphological aspect, with the formation of particles in the form of irregular polyhedral. These resulted from the applied temperature which represents a determining factor for the crystallinity of the material [24]. Coelho et al. [9] pointed out that, increasing the temperature, particles tend to coalesce leading to morphologies of polyhedral irregular shapes. Temperatures up to 1100 °C also contribute to the formation of hexagonal shape particles and plate type. These morphologies are an indication of delafossite phase formation. Similar results are presented in the literature [21, 25].

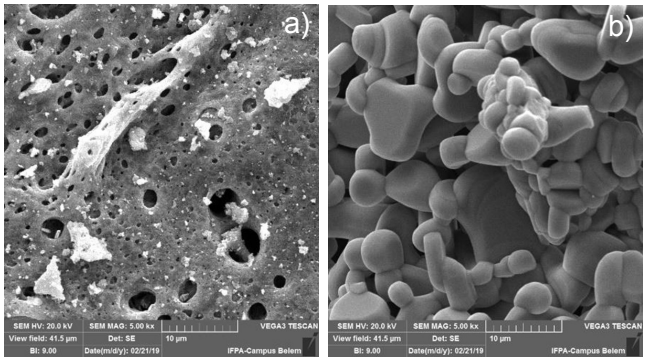

Figure 3: SEM micrographs of $CuCrO_2$ compound samples before, NC (a), and after, CC (b), heat treatment.

Infrared spectroscopy (IR): through infrared analysis, information about the bonds and functional groups present in the compound ($CuCrO_2$) was obtained. The infrared spectra of the non-calcined and calcinated material at 1100 °C are shown in Fig. 4. $CuCrO_2$-NC and $CuCrO_2$-CC samples exhibited similar spectral profiles. The bands of strong intensity located at 552 and 730 cm^{-1} were associated with the vibrational frequencies of Cu-O and Cr^{III}-O bonds, respectively [19, 26]. At 946 cm^{-1}, the stretching band present was related to the Cr^{IV}-O bonds [27]. According to Ahmad et al. [27], the presented absorption bands in these regions are characteristic of the $CuCrO_2$ phase. In the $CuCrO_2$-FC sample, there was a slight deviation of the bands in relation to the other spectral profiles. This behavior may be related to the presence of acidic functional groups in the structure of the $CuCrO_2$ compound. Functional groups from organic compounds were not detected, indicating that the

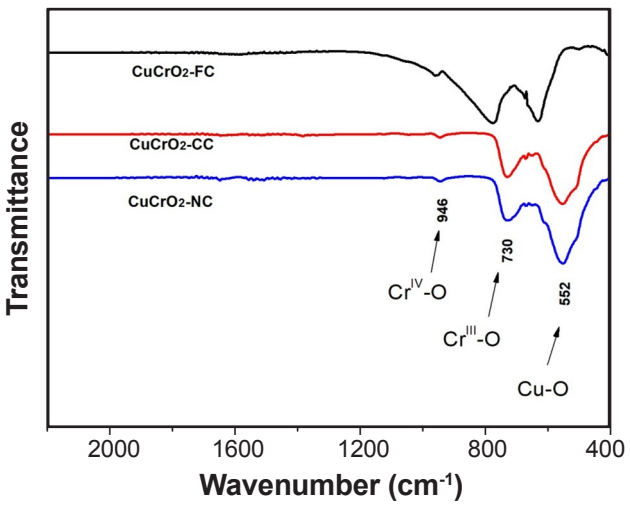

Figure 4: Infrared spectra of the $CuCrO_2$ compounds.

urea used as fuel during the synthesis of the specimens was entirely consumed during combustion, with the consequent formation of gases.

Catalytic test: this test was carried out in order to evaluate the efficiency of the compound $CuCrO_2$ as a catalyst in the ethyl transesterification reaction of soybean oil. The tests were performed with a $CuCrO_2$-FC sample with an alcohol:oil ratio of 12:1 at 150 °C for 6 h. In the reaction, ethyl esters were produced using the functionalized catalyst ($CuCrO_2$-FC). The results of the chromatographic analysis of this reaction are shown in Fig. 5. The chromatogram was characteristic of the soybean biodiesel pattern [27, 28]. The highest intensity peaks were related to the ethyl palmitate ester (peak 1), ethyl stearate (peak 3), ethyl oleate (peak 4), ethyl linoleate (peak 6), and ethyl linolenate (peak 9). The contents of these esters and other information are shown in Table II. Among the major esters, it was observed that ethyl linoleate was the main constituent (40%, T_r=20.94 min), followed by ethyl oleate (25%, T_r=19.79 min), ethyl palmitate (14%, T_r=14.83 min), ethyl linolenate (8.76%, T_r=22.37 min), and ethyl stearate (6.64%, T_r=19.32 min).

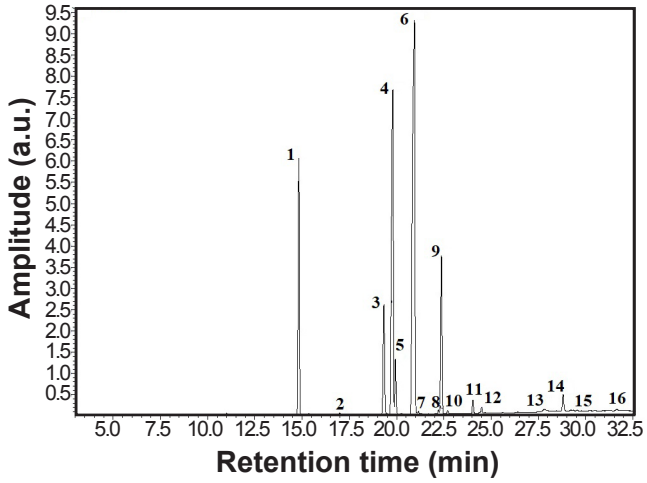

Figure 5: Chromatogram of soybean oil biodiesel.

Table II - Obtained ethyl esters in soybean biodiesel from the transesterification reaction and their characteristics.

Fatty acid ester	N° of carbon	$T_{retention}$ (min)	Composition (%)
Ethyl palmitate	C 16:0	14.83	14.0
Ethyl stearate	C 18:0	19.32	6.6
Ethyl oleate	C 18:1	19.79	25.0
Ethyl linoleate	C 18:2	20.94	40.0
Ethyl linolenate	C 18:3	22.37	8.8

These data agreed with other studies found in the literature [11, 29, 30]. Soybean biodiesel is characterized by the predominance of esters derived from unsaturated fatty acids.

The yield was calculated using Eq. A. In the reaction, 46 g (50 mL) of soybean oil was initially used. At the end of the reaction, 37 g (42 mL) of biodiesel was obtained and reached a yield of 80%. The yield value was considered satisfactory since the highest yields are achieved with basic catalysts in the methanolic reaction of vegetable oils. Other studies have reported similar results, such as Quintella et al. [31] who used mesoporous silica as a heterogeneous catalyst in the ethyl transesterification of soybean oil. In their investigation, 1% catalyst mass and 20:1 alcohol:oil molar ratio were employed in which 80% yield was obtained after 6 h of reaction at 100 °C. Yuan et al. [32] developed acid-based carbon catalysts which are utilized in the transesterification of soybean oil. In this research, an 8:1 molar ratio of ethanol to oil, 7% of catalyst, and a reaction period of 8 h at 80 °C were employed. As a result, there was a 70% conversion into ethyl esters. In contrast, for the non-calcined ($CuCrO_2$-NC) and calcined ($CuCrO_2$-CC) samples under the same reaction conditions (alcohol:oil ratio of 12:1 at 150 °C for 6 h), satisfactory reaction results were not possible and no conversion occurred. This result suggested that the pure delafossite compound does not perform as a catalyst for the transesterification reaction. The functionalization of the catalysts was essential for the conversion process, which can be associated with the modification of the structure and surface of the solid product. Additionally, it raises the acid character, removes impurities, and decreases hydrophobicity, thus increasing its catalytic activity for the transesterification reaction [33-35].

CONCLUSIONS

Combustion synthesis followed by calcination proved to be an efficient process to produce delafossite $CuCrO_2$. The results of the thermogravimetric analysis showed that the phase of the compound $CuCrO_2$ was stable up to 1000 °C. This observation was confirmed by the XRD analysis, which revealed that after the synthesis process, the obtained compound presented a mixture of oxides and after calcination, it exhibited greater crystallinity. The predominance of the $CuCrO_2$ crystalline phase was revealed by the well-defined peaks and their intensities. Porous morphology was presented

when the compound did not experience thermal treatment and irregularly shaped polygons were obtained when treated at 1100 °C. Absorption bands associated with the main connections of the delafossite were identified through the infrared spectra which characterized the formation of the oxide. The chromatographic analysis confirmed the conversion of soybean oil into biodiesel, with a yield of 80%. This revealed that the acidification process increased the activity of the catalyst, resulting in a good reaction yield.

ACKNOWLEDGMENTS

To IFMA for the financial support through the Public Notice PRPGI n° 106 (Selection of Student Dissertation Projects Linked to the IFMA *Stricto Sensu* Graduate Program), to FAPEMA for granting a scholarship and project financing, to the Fuel, Catalysis and Environmental Nucleus and to the Central Analítica of UFMA, for carrying out the analyzes and Prof. Cáritas Mendonça, Ph.D., from UFMA, for their collaboration from chromatographic analysis test.

REFERENCES

[1] S. Kumar, S. Marinel, M. Miclau, C. Martin, Mater. Lett. **70** (2012) 40.
[2] M.A. Marquardt, N.A. Ashmore, D.P. Cann, Thin Solid Films **496** (2006) 146.
[3] J.F.H. Monteiro, A.R. Jurelo, F.C. Monteiro, D.R. Mosca, Ceram. Int. **44** (2018) 14101.
[4] H.F. Jiang, C.Y. Gui, Y.Y. Zhu, D.J. Wu, S.P. Sun, C. Xiong, X.B. Zhu, J. Alloys Compd. **582** (2014) 64.
[5] A.P. Amrute, Z. Lodziana, C. Mondelli, F. Krumeich, J.P. Ramírez, Chem. Mater. **25** (2013) 4423.
[6] C. Taddee, T. Kamwanna, V. Amornkitbamrung, Appl. Surf. Sci. **380** (2016) 237.
[7] J. Wang, P. Zheng, D. Li, Z. Deng, W. Dong, R. Tao, X. Fang, J. Alloys Compd. **509** (2011) 5715.
[8] B.R. Vahid, M. Haghighi, Energy Convers. Manag. **126** (2016) 362.
[9] M.B.M. Coelho, M.M. Oliveira, I.C. Nogueira, J.H.G. Rangel, J.S. Vasconcelos, E. Azevedo, A.P. Maciel, E. Longo, Cerâmica **64**, 369 (2018) 49.
[10] M.E. Borges, L. Díaz, Renew. Sust. Energ. Rev. **16** (2012) 2839.
[11] C. Kordulis, K. Bourikas, M. Gousi, E. Kordouli, A. Lycourghiotis, Appl. Catal. B **18** (2016) 156.
[12] R.A. Ferrari, V.S. Oliveira, A. Scabio, Quim. Nova **28** (2005) 19.
[13] G.F. Ghesti, J.L. de Macedo, J.A. Dias, S.C.L. Dias, Quim. Nova **35** (2012) 119.
[14] T.C. dos Santo, E.C.S. Santos, J.P. Dias, J. Barreto, F.L. Stavale, C.M. Ronconi, Fuel **256** (2019) 115793.
[15] Y. Nian, H. Teng, J. Electrochem. Soc. **8** (2002) 149.
[16] Y. Zhong, Q. Deng, P. Zhang, J. Wang, R. Wang, Z. Zeng, S. Deng, Fuel **240** (2019) 270.
[17] J.L. Figueiredo, J. Mater. Chem. A **1** (2013) 9351.
[18] W. Ketir, G. Rekhila, M. Trari, A. Amrane. J. Environ. Sci. **24** (2012) 2173.
[19] D. Ursu, M. Miclau, J. Nanopart. Res. **16** (2014) 2160.
[20] W. Li, H. Cheng, J. Cent. South Univ. Technol. **14** (2007) 291.
[21] F.D.A.B.L. Martins, M.B.M. Coelho, R.N.R.D. Silva, J.S. Vasconcelos, J.H.G. Rangel, E. Longo, J.M.R. Mercury, Matéria **24** (2019) 24.
[22] A. Figarol, J. Pourchez, D. Boudard, V. Forest, J.M. Tulliani, J.P. Lecompte, P. Grosseau, J. Nanopart. Res. **16** (2014) 2507.
[23] E.L. Foletto, C. Volzone, A.F. Morgado, L.M. Porto, Cerâmica **47**, 304 (2001) 208.
[24] J.F.H.L. Monteiro, A.R. Jurelo, E.C. Siqueira, Solid State Commun. **252** (2017) 64.
[25] Z.Y. Liu, G.Y. Wang, X.P. Liu, Y.J. Wang. J. Fuel Chem. Technol. **41** (2013) 1473.
[26] Y.H. Chuai, X. Wang, H.Z. Shen, Y.D. Li, C.T. Zheng, Y.D. Wang, J. Mater. Sci. **51** (2016) 3592.
[27] T. Ahmad, R. Phul, P. Alam, I.H. Lone, M. Shahazad, J. Ahmed, S.M. Alshehri, RSC Adv. **7** (2017) 27549.
[28] M. Stefanescu, M. Barbu, T. Vlase, P. Barvinschi, L. Barbu-Tudoran, M. Stoia, Thermochim. Acta **526** (2011) 130.
[29] S.T. Keera, S.M. El Sabagh, A.R. Taman, Fuel **90** (2017) 42.
[30] M.V. Marques, F.F. Naciuk, A.M.D.S. Mello, N.M. Seibel, L.A.M. Fontoura, Quím. Nova **33** (2010) 978.
[31] S.A. Quintella, R.M. Saboya, D.C. Salmin, D.S. Novaes, A.S. Araújo, M.C. Albuquerque, C.L. Cavalcante, Renew. Energ. **38** (2012) 136.
[32] L. Yuan, X.L. Zhang, W.Y. Gao, L.G. Ren, J. Liaoning Univ. Petrol. Chem. Technol. **2** (2018) 156.
[33] C.M. Garcia, S. Teixeira, L.L. Marciniuk, U. Schuchardt, Bioresour. Technol. **14** (2008) 6608.
[34] D. Zuo, J. Lane, D. Culy, M. Schultz, A. Pullar, M. Waxman, Appl Catal. B **129** (2013) 342.
[35] M. Ramos, A.P.S. Dias, J.F. Puna, J. Gomes, J.C. Bordado, Energies **12** (2019) 4408.
(Rec. 26/03/2022, Rev. 14/09/2022, Ac. 11/10/2022)

CC BY-NC